Optical coupled-mode theory for dielectric solids of revolution

E. N. Bulgakov [1,2] D. N. Maksimov, [1,2,3] and A. E. Ershov [1,3]

[1]*Institute of Computational Modeling SB RAS, Krasnoyarsk 660036, Russia*
[2]*Kirensky Institute of Physics, Federal Research Center KSC SB RAS, Krasnoyarsk 660036, Russia*
[3]*IRC SQC, Siberian Federal University, Krasnoyarsk 660041, Russia*

We propose a single resonance coupled-mode approach to light scattering by dielectric solids of revolution. By using a biorthogonal decomposition of the *S* matrix found with the extended boundary condition method we derived all parameters required for application of the temporal coupled-mode theory in a closed form. The proposed approach allows for constructing a frequency-dependent Fano response due to a single resonance after the full-wave solution has been found at a single incident frequency.

I. INTRODUCTION

Dielectric nanoparticles made of high-index materials are currently thought of as an efficient instrument for engineering an optical response [1–5]. Typically, the optical response of such particles exhibits a sequence of Fano features [6–8] which are due to coupling between the incident light and high-quality resonant modes. Therefore, it appears very natural to employ the modal expansions of electromagnetic field using the resonant eigenmodes as a set of basis functions. This idea has led to a variety of techniques known as resonant (quasinormal) state expansion methods [9–12]. In addition to the necessity of first calculating the resonant modes, these methods face the difficulty of eigenmode divergence in the far zone, that can be coped with by introducing specific normalization conditions [13]. Alternatively, utilizing constant flux states [14] or the Fano-Feshbach projection technique with closed-cavity eigenmodes [15] is possible for solving the scattering problem via a modal decomposition.

Another approach for describing the optical response in terms of a resonance is known as the temporal coupled-mode theory (TCMT) [16]. The key idea behind the TCMT is to map the scattering problem onto a lossy driven oscillator. Technically, the TCMT approach leads to an ordinary differential equation which is easily solved in the time-harmonic regime. It occurs in the TCMT framework that the coefficients of the dynamic model are not independent but must satisfy three constraints imposed by symmetry and energy conservation [17]. These constraints dramatically simplify application of the TCMT, making it an efficient tool for fitting the scattering spectra. The TCMT can be generalized to the multimodal case leading to a system of ordinary differential equations [18] as well as applied in the multichannel case with infinitely many scattering channels [19].

Numerous attempts have been made to establish a link between the TCMT and rigorous full-wave simulation methods [11,20–28]. So far, the most promising approaches relied on quasinormal mode expansions [12,21,23,28,29]. In these methods one applies the eigenmodes of a non-Hermitian Maxwell operator which have to be either computed or known

analytically beforehand. Here, we take a different route. By using the extended boundary condition method (EBCM) [30] we derive all TCMT parameters from the biorthogonal decomposition of the *S* matrix without first solving the eigenvalue problem for Maxwell's equations. In this paper we construct a single-mode TCMT for light scattering by lossless dielectric solids of revolution (SR) which pose a challenge due an infinite number of scattering channel. The paper is organized as follows. In Sec. II we discuss the generic properties of the TCMT model for the SR. In Sec. III we review the EBCM method. In Sec. IV we employ biorthogonal decomposition to derive the TCMT parameters. The TCMT resonant mode and total solution for the electromagnetic field are derived in Sec. V. In Sec. VI we summarize our findings and provide numerical examples for validation of the theory. Finally, we conclude in Sec. VII.

II. TCMT FOR SOLIDS OF REVOLUTION

Let us consider a dielectric solid of revolution as shown in Fig. 1. To construct the coupled-mode theory we start from the far-field solution written in the following form,

$$
\boldsymbol{E}_{\text{tot}} = \sum_{\ell=1}^{\infty} \sum_{m=-\ell}^{\ell} \big[a_{\ell,m}^{(+)} \boldsymbol{M}_{\ell,m}^{(2)}(k_0, \boldsymbol{r}) + b_{\ell,m}^{(+)} \boldsymbol{N}_{\ell,m}^{(2)}(k_0, \boldsymbol{r})
$$
$$
+ a_{\ell,m}^{(-)} \boldsymbol{M}_{\ell,m}^{(3)}(k_0, \boldsymbol{r}) + b_{\ell,m}^{(-)} \boldsymbol{N}_{\ell,m}^{(3)}(k_0, \boldsymbol{r}) \big], \tag{1}
$$

where $\boldsymbol{M}_{\ell,m}^{(j)}$ and $\boldsymbol{N}_{\ell,m}^{(j)}$ are magnetic and electric vector spherical harmonics, correspondingly. The case $j = 2$ corresponds to incident harmonics while $j = 3$ stands for their outgoing counterparts. Below we write down the major TCMT equations along the same line as in Ref. [19]. The dynamic equation for amplitude a of the resonant mode reads

$$
\frac{da}{dt} = (-i\omega_0 - \gamma)a + \boldsymbol{\kappa}^{\mathsf{T}} \mathbf{a}_{(+)}, \tag{2}
$$

where ω_0 is the resonant eigenfrequency, γ the radiation decay rate, $\boldsymbol{\kappa}$ the incident coupling vector, and $\mathbf{a}_{(+)}$ is a vector of incident amplitudes. The vector of outgoing amplitudes $\mathbf{a}_{(-)}$
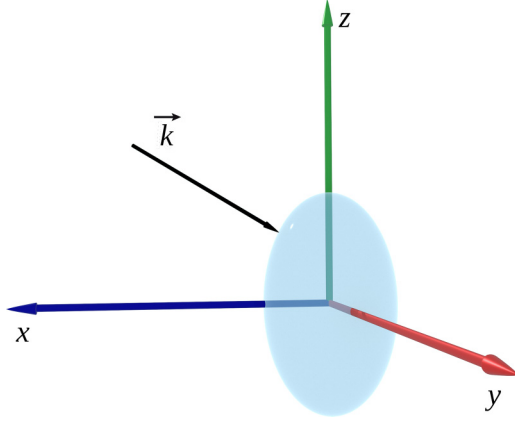
FIG. 1. Dielectric solid of revolution. The particle is symmetric to rotation about the z axis.

can be found from the second TCMT equation

$$\mathbf{a}_{(-)} = \widehat{B}\mathbf{a}_{(+)} + a\mathbf{d}, \tag{3}$$

where $\widehat{B}$ is the matrix of a direct (nonresonant) process, and $\mathbf{d}$ is the outgoing coupling vector. The S matrix is implicitly defined as

$$\mathbf{a}_{(-)} = \widehat{S}\mathbf{a}_{(+)}. \tag{4}$$

Here, we adopt the following notations to define the vectors of incident and outgoing amplitudes. First, let us define

$$\mathbf{a}_m^{(\pm)} = \left(a_{\ell_0,m}^{(\pm)}, \ldots, a_{\ell,m}^{(\pm)}, \ldots, b_{\ell_0,m}^{(\pm)}, \ldots, b_{\ell,m}^{(\pm)}, \ldots\right)^{\mathsf{T}},$$

$$\ell_0 = \begin{cases} 1, & \text{if } m = 0, \\ |m|, & \text{if } m \neq 0, \end{cases} \tag{5}$$

and then

$$\mathbf{a}_{(\pm)}^{\mathsf{T}} = \left(\mathbf{a}_{-\infty}^{(\pm)}{}^{\mathsf{T}}, \ldots \mathbf{a}_m^{(\pm)}{}^{\mathsf{T}}, \mathbf{a}_{m+1}^{(\pm)}{}^{\mathsf{T}}, \ldots \mathbf{a}_\infty^{(\pm)}{}^{\mathsf{T}}\right). \tag{6}$$

Given that for the SR the projection of the angular momentum onto the z axis is preserved, the S matrix must have a block form. This allows us to build a TCMT model for each m independently using the following definition of the S matrix,

$$\mathbf{a}_m^{(-)} = \widehat{S}_m \mathbf{a}_m^{(+)}. \tag{7}$$

In what follows we will use the subscript m to emphasize that all quantities are defined for a specific value of m. The total vector and matrix quantities used in Eqs. (2) and (3) can be constructed according to the rules applied in Eq. (6).

The parameters in Eqs. (2) and (3) are not independent [16]. By applying time-reversal, symmetry, and energy conservation arguments it is possible to establish some useful relationships between $\widehat{B}_m$, $\boldsymbol{\kappa}_m$, $\mathbf{d}_m$, and γ. Notice though that care is needed when applying the time-reversal operator [19]. The time-reversal operation transforms an outgoing (incoming) wave in the channel m to an incoming (outgoing) wave in the channel $-m$. Thus, for the time reversal of the amplitude vector $\mathbf{a}_m^{(\pm)}$ we have

$$\mathcal{T}\mathbf{a}_m^{(\pm)} = (\mathbf{a}_{-m}^{(\mp)})^*, \tag{8}$$

which together with the unitarity of the S matrix leads to

$$\widehat{S}_m^{\mathsf{T}} = \widehat{S}_{-m}. \tag{9}$$

At the same time let us employ the σ_v operation which corresponds to the symmetry with respect to changing the sign of the azimuthal variable $\phi \to -\phi$. Under the action of σ_v we have

$$\boldsymbol{M}_{\ell,m}(\phi) \xrightarrow{\sigma_v} (-1)^{m+1}\boldsymbol{M}_{\ell,-m}(\phi),$$

$$\boldsymbol{N}_{\ell,m}(\phi) \xrightarrow{\sigma_v} (-1)^m \boldsymbol{N}_{\ell,-m}(\phi), \tag{10}$$

which leads to

$$\widehat{S}_m = \widehat{J}\widehat{S}_{-m}\widehat{J}, \tag{11}$$

where

$$\widehat{J} = \begin{pmatrix} -\widehat{\mathbb{1}} & 0 \\ 0 & \widehat{\mathbb{1}} \end{pmatrix}, \tag{12}$$

with the upper row acting on $a_{\ell,m}^{(\pm)}$, the lower row acting on $b_{\ell,m}^{(\pm)}$, and $\widehat{\mathbb{1}}$ being the identity matrix. Combining Eqs. (9) and (11) we have

$$\widehat{S}_m^{\mathsf{T}} = \widehat{J}\widehat{S}_m\widehat{J}, \tag{13}$$

Next, by considering the radiative decay [16,19] one can find from Eqs. (2) and (3) in the absence of an incident wave

$$\frac{d|a|^2}{dt} = -2\gamma|a|^2 = -(\mathbf{a}_m^{(-)})^\dagger \mathbf{a}_m^{(-)} = -\mathbf{d}_m^\dagger \mathbf{d}_m |a|^2, \tag{14}$$

and thus

$$\mathbf{d}_m^\dagger \mathbf{d}_m = 2\gamma. \tag{15}$$

Further on, the time-reversal operation is typically applied [16,19] to Eqs. (2) and (3) for finding two extra relationships between the TCMT parameters. We, however, already applied the time reversal for deriving Eq. (13) and restricted our approach to a fixed value of m. For deriving the rest of the TCMT relationships we have to take a different route by using Eq. (13) together with the unitarity of the S matrix. The derivation is now somewhat cumbersome and therefore presented in the Appendix. Nonetheless, the results are very similar to those reported in Ref. [19], namely,

$$\widehat{B}_m\widehat{J}\mathbf{d}_m^* + \mathbf{d}_m = 0, \tag{16}$$

and

$$\boldsymbol{\kappa}_m = \widehat{J}\mathbf{d}_m. \tag{17}$$

Finally, the time-stationary solution for the S matrix at incident frequency ω can be written as

$$\widehat{S}_m = \widehat{B}_m + \frac{\mathbf{d}_m\mathbf{d}_m^{\mathsf{T}}\widehat{J}}{i\omega_0 - i\omega + \gamma}. \tag{18}$$

III. EBCM METHOD

For constructing TCMT we shall apply the approach of the transition matrix (T matrix). Practically, one of the most efficient formulations of the T-matrix approach is the extended boundary condition (EBCM) method [31]. In the EBCM framework the electromagnetic field, both incident and reflected, is expanded into spherical vector harmonics. In the

surrounding medium (air) we can write for the incident field

$$\boldsymbol{E}_{\text{in}} = \sum_{\ell=1}^{\infty} \sum_{m=-\ell}^{\ell} \left[a_{\ell,m} \boldsymbol{M}_{\ell,m}^{(1)}(k_0, \boldsymbol{r}) + b_{\ell,m} \boldsymbol{N}_{\ell,m}^{(1)}(k_0, \boldsymbol{r}) \right], \quad (19)$$

where k_0 is the vacuum wave number. Inside the SR we write

$$\boldsymbol{E}_{\text{SR}} = \sum_{\ell=1}^{\infty} \sum_{m=-\ell}^{\ell} \left[c_{\ell,m} \boldsymbol{M}_{\ell,m}^{(1)}(k', \boldsymbol{r}) + d_{\ell,m} \boldsymbol{N}_{\ell,m}^{(1)}(k', \boldsymbol{r}) \right], \quad (20)$$

where $k' = \sqrt{\epsilon} k_0$. The scattered field outside the SR is written as

$$\boldsymbol{E}_{\text{sc}} = \sum_{\ell=1}^{\infty} \sum_{m=-\ell}^{\ell} \left[p_{\ell,m} \boldsymbol{M}_{\ell,m}^{(3)}(k_0, \boldsymbol{r}) + q_{\ell,m} \boldsymbol{N}_{\ell,m}^{(3)}(k_0, \boldsymbol{r}) \right]. \quad (21)$$

The unknown expansion coefficient $c_{\ell,m}$, $d_{\ell,m}$ can be found from $a_{\ell,m}$, $b_{\ell,m}$ by solving a system of linear equations

$$-i a_{\ell',m'} = \sum_{\ell=1}^{\infty} \sum_{m=-\ell}^{\ell} \left(\sqrt{\epsilon} J_{\ell',m'}^{\ell,m} + K_{\ell',m'}^{\ell,m} \right) c_{\ell,m}$$

$$+ \sum_{\ell=1}^{\infty} \sum_{m=-\ell}^{\ell} \left(\sqrt{\epsilon} I_{\ell',m'}^{\ell,m} + L_{\ell',m'}^{\ell,m} \right) d_{\ell,m},$$

$$-i b_{\ell',m'} = \sum_{\ell=1}^{\infty} \sum_{m=-\ell}^{\ell} \left(\sqrt{\epsilon} L_{\ell',m'}^{\ell,m} + I_{\ell',m'}^{\ell,m} \right) c_{\ell,m}$$

$$+ \sum_{\ell=1}^{\infty} \sum_{m=-\ell}^{\ell} \left(\sqrt{\epsilon} K_{\ell',m'}^{\ell,m} + J_{\ell',m'}^{\ell,m} \right) d_{\ell,m}. \quad (22)$$

The system's coefficients are found as integrals over the SR surface,

$$I_{\ell',m'}^{\ell,m} = k_0^2 \int dS \, \mathbf{n} \cdot \left[\boldsymbol{M}_{\ell',m'}^{(3)*}(k_0, \boldsymbol{r}) \times \boldsymbol{M}_{\ell,m}^{(1)}(k', \boldsymbol{r}) \right],$$

$$J_{\ell',m'}^{\ell,m} = k_0^2 \int dS \, \mathbf{n} \cdot \left[\boldsymbol{M}_{\ell',m'}^{(3)*}(k_0, \boldsymbol{r}) \times \boldsymbol{N}_{\ell,m}^{(1)}(k', \boldsymbol{r}) \right],$$

$$K_{\ell',m'}^{\ell,m} = k_0^2 \int dS \, \mathbf{n} \cdot \left[\boldsymbol{N}_{\ell',m'}^{(3)*}(k_0, \boldsymbol{r}) \times \boldsymbol{M}_{\ell,m}^{(1)}(k', \boldsymbol{r}) \right],$$

$$L_{\ell',m'}^{\ell,m} = k_0^2 \int dS \, \mathbf{n} \cdot \left[\boldsymbol{N}_{\ell',m'}^{(3)*}(k_0, \boldsymbol{r}) \times \boldsymbol{N}_{\ell,m}^{(1)}(k', \boldsymbol{r}) \right], \quad (23)$$

where $\mathbf{n}$ is the unit vector normal to the surface of the SR. Once Eq. (22) is solved for $c_{\ell,m}$, $d_{\ell,m}$, the unknowns $p_{\ell,m}$, $q_{\ell,m}$ can be found from the equations

$$p_{\ell',m'} = \sum_{\ell=1}^{\infty} \sum_{m=-\ell}^{\ell} \left(-i\sqrt{\epsilon} \tilde{J}_{\ell',m'}^{\ell,m} - i\tilde{K}_{\ell',m'}^{\ell,m} \right) c_{\ell,m}$$

$$+ \sum_{\ell=1}^{\infty} \sum_{m=-\ell}^{\ell} \left(-i\sqrt{\epsilon} \tilde{I}_{\ell',m'}^{\ell,m} - i\tilde{L}_{\ell',m'}^{\ell,m} \right) d_{\ell,m},$$

$$q_{\ell',m'} = \sum_{\ell=1}^{\infty} \sum_{m=-\ell}^{\ell} \left(-i\sqrt{\epsilon} \tilde{L}_{\ell',m'}^{\ell,m} - i\tilde{I}_{\ell',m'}^{\ell,m} \right) c_{\ell,m}$$

$$+ \sum_{\ell=1}^{\infty} \sum_{m=-\ell}^{\ell} \left(-i\sqrt{\epsilon} \tilde{K}_{\ell',m'}^{\ell,m} - i\tilde{J}_{\ell',m'}^{\ell,m} \right) d_{\ell,m}, \quad (24)$$

where the coefficients are given by

$$\tilde{I}_{\ell',m'}^{\ell,m} = k_0^2 \int dS \, \mathbf{n} \cdot \left[\boldsymbol{M}_{\ell',m'}^{(1)*}(k_0, \boldsymbol{r}) \times \boldsymbol{M}_{\ell,m}^{(1)}(k', \boldsymbol{r}) \right],$$

$$\tilde{J}_{\ell',m'}^{\ell,m} = k_0^2 \int dS \, \mathbf{n} \cdot \left[\boldsymbol{M}_{\ell',m'}^{(1)*}(k_0, \boldsymbol{r}) \times \boldsymbol{N}_{\ell,m}^{(1)}(k', \boldsymbol{r}) \right],$$

$$\tilde{K}_{\ell',m'}^{\ell,m} = k_0^2 \int dS \, \mathbf{n} \cdot \left[\boldsymbol{N}_{\ell',m'}^{(1)*}(k_0, \boldsymbol{r}) \times \boldsymbol{M}_{\ell,m}^{(1)}(k', \boldsymbol{r}) \right],$$

$$\tilde{L}_{\ell',m'}^{\ell,m} = k_0^2 \int dS \, \mathbf{n} \cdot \left[\boldsymbol{N}_{\ell',m'}^{(1)*}(k_0, \boldsymbol{r}) \times \boldsymbol{N}_{\ell,m}^{(1)}(k', \boldsymbol{r}) \right]. \quad (25)$$

The power of the outgoing radiation can be found as

$$P = \frac{k_0^2}{2} \sum_{\ell=1}^{\infty} \sum_{m=-\ell}^{\ell} (|p_{\ell,m}|^2 + |q_{\ell,m}|^2), \quad (26)$$

while the energy conservation leads to

$$\sum_{\ell=1}^{\infty} \sum_{m=-\ell}^{\ell} (|p_{\ell,m}|^2 + |q_{\ell,m}|^2 + \text{Re}\{p_{\ell,m} a_{\ell,m}^*\} + \text{Re}\{q_{\ell,m} b_{\ell,m}^*\}) = 0. \quad (27)$$

The T matrix links the incident and outgoing amplitudes

$$\mathbf{a}_m^{(\text{out})} = \widehat{T}_m \mathbf{a}_m^{(\text{in})}, \quad (28)$$

where $\mathbf{a}_m^{(\text{in})}$ and $\mathbf{a}_m^{(\text{out})}$ are assembled of the expansion coefficients $a_{\ell,m}$, $b_{\ell,m}$ in Eq. (19) and $p_{\ell,m}$, $q_{\ell,m}$ in Eq. (21), correspondingly, according to the rules defined in Eq. (5). For further convenience we introduce vector $\mathbf{c}_m$ assembled from $c_{\ell,m}$ and $d_{\ell,m}$ according to the same rules. Then, Eqs. (22) and (24) can be rewritten in a matrix form,

$$-i\mathbf{a}_m^{(\text{in})} = \widehat{M}_m \mathbf{c}_m, \quad \mathbf{a}_m^{(\text{out})} = \widehat{N}_m \mathbf{c}_m. \quad (29)$$

As we have defined in Sec. II, the scattering channels in the TCMT approach are incident $\boldsymbol{M}_{\ell,m}^{(2)}$, $\boldsymbol{N}_{\ell,m}^{(2)}$ and $\boldsymbol{M}_{\ell,m}^{(3)}$, $\boldsymbol{N}_{\ell,m}^{(3)}$ outgoing spherical harmonics. Therefore the vectors of incident and outgoing amplitudes are given by

$$\mathbf{a}_m^{(+)} = \tfrac{1}{2} \mathbf{a}_m^{(\text{in})}, \quad \mathbf{a}_m^{(-)} = \mathbf{a}_m^{(\text{out})} + \tfrac{1}{2} \mathbf{a}_m^{(\text{in})}. \quad (30)$$

By combining Eqs. (28) and (30) one finds

$$\widehat{S}_m = \widehat{\mathbb{1}} + 2\widehat{T}_m. \quad (31)$$

The formal solutions for the S matrix read

$$\widehat{S}_m = \widehat{\mathbb{1}} - 2i\widehat{N}_m \widehat{M}_m^{-1}. \quad (32)$$

IV. CALCULATION OF THE TCMT PARAMETERS

According to Eq. (18) the resonant contribution in the S matrix reads

$$\widehat{S}_m^{(\text{res})} = \frac{\mathbf{d}_m \mathbf{d}_m^{\mathsf{T}} \widehat{J}}{i\omega_0 - i\omega + \gamma}. \quad (33)$$

To calculate the resonant term we use the biorthogonal basis [32] of the left and right eigenvectors of matrix $\widehat{M}_m$ at incident frequency ω,

$$\widehat{M}_m \boldsymbol{x}_n = \lambda_n \boldsymbol{x}_n, \quad \widehat{M}_m^\dagger \boldsymbol{y}_n = \lambda_n^* \boldsymbol{y}_n. \quad (34)$$

The basis vectors satisfy the following normalization condition,

$$\mathbf{y}_n^\dagger \mathbf{x}_{n'} = \delta_{n,n'}, \tag{35}$$

while the closure condition reads

$$\widehat{\mathbb{I}} = \sum_{n=1}^{\infty} \mathbf{x}_n \mathbf{y}_n^\dagger. \tag{36}$$

By virtue of Eqs. (35) and (36) we can write

$$\widehat{M}_m^{-1} = \sum_{n=1}^{\infty} \frac{1}{\lambda_n} \mathbf{x}_n \mathbf{y}_n^\dagger. \tag{37}$$

Then, for the S matrix we have

$$\widehat{S}_m = \widehat{\mathbb{I}} - 2i\widehat{N}_m(\omega) \sum_{n=1}^{\infty} \frac{1}{\lambda_n(\omega)} \mathbf{x}_n(\omega) \mathbf{y}_n^\dagger(\omega), \tag{38}$$

where we emphasized the frequency dependence of the biorthogonal expansion.

At this point we hypothesize that the resonant feature in the optical response at certain frequency $\bar{\omega}$ is due to the smallest (resonant) eigenvalue of $\widehat{M}_m$. To justify the hypothesis we point out that near a high-quality resonance we expect a pole of the S matrix near the real axis. The matrix $\widehat{N}_m(\omega)$ is nonsingular by construction while the eigenvectors are normalized. Therefore, only vanishing λ_n can lead to singularity. Thus, we can write

$$\widehat{S}_m^{(\mathrm{res})} = -2i\widehat{N}_m(\omega) \frac{\mathbf{x}_r(\omega) \mathbf{y}_r^\dagger(\omega)}{\lambda_r(\omega)}, \tag{39}$$

and

$$\widehat{B}_m = \widehat{\mathbb{I}} - 2i\widehat{N}_m(\bar{\omega}) \sum_{n \neq r}^{\infty} \frac{1}{\lambda_n(\bar{\omega})} \mathbf{x}_n(\bar{\omega}) \mathbf{y}_n^\dagger(\bar{\omega}). \tag{40}$$

Notice that, in accordance with the TCMT, in the above expressions we assumed that only the resonant term $\widehat{S}_m^{(\mathrm{res})}$ is dependent on ω, whereas the rest of the resonant contributions into Eq. (38) can be taken constant in the frequency range of interest. Since now Eq. (39) is the only frequency-dependent term, by using Eq. (13) one finds

$$\widehat{N}_m(\omega) \mathbf{x}_r(\omega) \mathbf{y}_r^\dagger(\omega) = \widehat{J} \mathbf{y}_r^*(\omega) \mathbf{x}_r^\mathsf{T}(\omega) \widehat{N}_m^\mathsf{T}(\omega) \widehat{J}. \tag{41}$$

By defining a new vector

$$\mathbf{z}_r(\omega) = \widehat{N}_m^*(\omega) \mathbf{x}_r^*(\omega), \tag{42}$$

one finds from Eq. (41)

$$\mathbf{z}_r(\omega) = \widehat{J} \mathbf{y}_r(\omega) \mathbf{x}_r^\dagger(\omega) \widehat{N}_m^\dagger(\omega) \widehat{J} \mathbf{x}_r^*(\omega). \tag{43}$$

Next, by using our definition of the biorthogonal basis vectors we find

$$\widehat{M}_m^\dagger(\omega) \widehat{J} \mathbf{z}_r(\omega) = \lambda_r^* \widehat{J} \mathbf{z}_r(\omega). \tag{44}$$

Thus, we have

$$\mathbf{y}_r(\omega) = u^* \widehat{J} \mathbf{z}_r(\omega), \tag{45}$$

where u is an unknown complex constant.

At the same time let us perform a Taylor expansion of λ_r in the vicinity of $\bar{\omega}$,

$$\lambda_r(\omega) = \lambda_r(\bar{\omega}) + \alpha(\bar{\omega} - \omega), \tag{46}$$

where

$$\alpha = -\left. \frac{\partial \lambda_r(\omega)}{\partial \omega} \right|_{\omega = \bar{\omega}} \tag{47}$$

By substituting Eqs. (42), (45), and (46) into Eq. (39) we write

$$\widehat{S}_m^{(\mathrm{res})} = -2iu \frac{\mathbf{z}_r^*(\bar{\omega}) \mathbf{z}_r^\dagger(\bar{\omega}) \widehat{J}}{\lambda_r(\bar{\omega}) + \alpha(\bar{\omega} - \omega)}, \tag{48}$$

where we neglected the frequency dependence in the numerator as required by the TCMT. By comparing Eq. (48) with Eq. (33) we find

$$\mathbf{d}_m = \sqrt{\frac{2u}{\alpha}} \mathbf{z}_r^*(\bar{\omega}), \tag{49}$$

and

$$\omega_0 = \bar{\omega} + \mathrm{Re}\left\{ \frac{\lambda_r(\bar{\omega})}{\alpha} \right\},$$

$$\gamma = -\mathrm{Im}\left\{ \frac{\lambda_r(\bar{\omega})}{\alpha} \right\}. \tag{50}$$

Finally, we can rewrite Eq. (49) with application of Eq. (45) as follows,

$$\mathbf{d}_m = \sqrt{\frac{2}{\alpha u}} \widehat{J} \mathbf{y}_r^*(\bar{\omega}). \tag{51}$$

By using $\mathbf{d}_m^\dagger \mathbf{d}_m = 2\gamma$ we find

$$|u| = \frac{\mathbf{y}_r^\mathsf{T}(\bar{\omega}) \mathbf{y}_r^*(\bar{\omega})}{|\alpha|\gamma}. \tag{52}$$

The above equations constitute the full set of formulas required for applying the TCMT decomposition of the scattering spectrum. All we need at this point is to check that the proposed theory satisfies all of the TCMT constraints, namely, Eqs. (15)–(17). Notice, though, that Eq. (15) is explicitly used in the construction of the theory and therefore is automatically satisfied. Equation (17) is satisfied by using it as the definition of $\boldsymbol{\kappa}_m$, i.e., $\boldsymbol{\kappa}_m = \widehat{J} \mathbf{d}_m$. Finally, the validity of Eq. (16) can be easily proven from the unitarity of the S matrix decomposed into resonant [Eq. (33)] and nonresonant [Eq. (40)] terms.

V. FIELD INSIDE THE SOLID OF REVOLUTION

Let us consider the TCMT solution for the electromagnetic field within the SR. The solution can be written as a sum of the resonant and direct contributions

$$\boldsymbol{E}_{\mathrm{SR}} = \boldsymbol{E}_{\mathrm{SR}}^{(\mathrm{res})} + \boldsymbol{E}_{\mathrm{SR}}^{(\mathrm{dir})}. \tag{53}$$

According to Eq. (20) the field $\boldsymbol{E}_{\mathrm{SR}}$ can be written in terms of its vector of expansion coefficient $\mathbf{c}_m$. From Eqs. (29) and (30) we have

$$\mathbf{c}_m = -2i\widehat{M}_m^{-1} \mathbf{a}_m^{(+)}. \tag{54}$$

In accordance with Eq. (53) we decompose Eq. (54) into direct and resonant contributions with an application of Eq. (37).

TABLE I. List of the TCMT formulas.

Resonant frequency	$\omega_0 = \bar{\omega} + \mathrm{Re}\{\frac{\lambda_r(\bar{\omega})}{\alpha}\}$
Radiative decay rate	$\gamma = -\mathrm{Im}\{\frac{\lambda_r(\bar{\omega})}{\alpha}\}$
Outgoing coupling vector	$\mathbf{d}_m = \sqrt{\frac{2\gamma}{\mathbf{y}_r^\dagger(\bar{\omega})\mathbf{y}_r(\bar{\omega})}}\widehat{J}\mathbf{y}_r^*(\bar{\omega})$
Incident coupling vector	$\kappa_m = \widehat{J}\mathbf{d}_m$
Resonant mode expansion	$\mathbf{c}_r = \frac{-2i}{\alpha}\sqrt{\frac{\mathbf{y}_r^\dagger(\bar{\omega})\mathbf{y}_r(\bar{\omega})}{2\gamma}}\mathbf{x}_r(\bar{\omega})$
Resonant mode amplitude	$a(\omega) = \frac{\kappa_m^\mathsf{T}}{i\omega_0 - i\omega + \gamma}\mathbf{a}_m^{(+)}$
Resonant field expansion	$\mathbf{c}_m^{(\mathrm{res})}(\omega) = a(\omega)\mathbf{c}_r$
Background field expansion	$\mathbf{c}_m^{(\mathrm{dir})} = \mathbf{c}_m(\omega) - \mathbf{c}_m^{(\mathrm{res})}(\bar{\omega})$
Total field expansion	$\mathbf{c}_m(\omega) = \mathbf{c}_m^{(\mathrm{dir})} + \mathbf{c}_m^{(\mathrm{res})}(\omega)$
Background S matrix	$\widehat{B}_m = \widehat{S}_m(\bar{\omega}) - \frac{\mathbf{d}_m \kappa_m^\mathsf{T}}{i\omega_0 - i\bar{\omega} + \gamma}$
Total S matrix	$\widehat{S}_m(\omega) = \widehat{B}_m + \frac{\mathbf{d}_m \kappa_m^\mathsf{T}}{i\omega_0 - i\omega + \gamma}$
Outgoing amplitudes	$\mathbf{a}_m^{(-)}(\omega) = \widehat{S}_m(\omega)\mathbf{a}_m^{(+)}$

The result reads

$$\mathbf{c}_m^{(\mathrm{dir})} = -2i\sum_{n\neq r}^{\infty}\frac{1}{\lambda_n}\mathbf{x}_n(\bar{\omega})\mathbf{y}_n^\dagger(\bar{\omega})\mathbf{a}_m^{(+)}, \tag{55}$$

and

$$\mathbf{c}_m^{(\mathrm{res})} = -2i\frac{\mathbf{x}_r(\bar{\omega})\mathbf{y}_r^\dagger(\bar{\omega})}{\lambda_r(\bar{\omega}) + \alpha(\bar{\omega} - \omega)}\mathbf{a}_m^{(+)}, \tag{56}$$

where in accordance with the TCMT we assumed that all quantities are independent of ω except λ_r which is written as the Taylor expansion Eq. (46). Let us rewrite Eq. (56) as follows with the use of Eq. (51),

$$\mathbf{c}_m^{(\mathrm{res})} = -i\sqrt{\frac{2u}{\alpha}}\frac{\mathbf{x}_r(\bar{\omega})\mathbf{d}_m^\mathsf{T}\widehat{J}}{i\omega_0 - i\omega + \gamma}\mathbf{a}_m^{(+)}. \tag{57}$$

At the same time the solution of Eq. (2) for the amplitude of the TCMT resonant mode reads

$$a = \frac{\mathbf{d}_m^\mathsf{T}\widehat{J}}{i\omega_0 - i\omega + \gamma}\mathbf{a}_m^{(+)}. \tag{58}$$

Finally, the expansion vector of the resonant contribution has to be written as

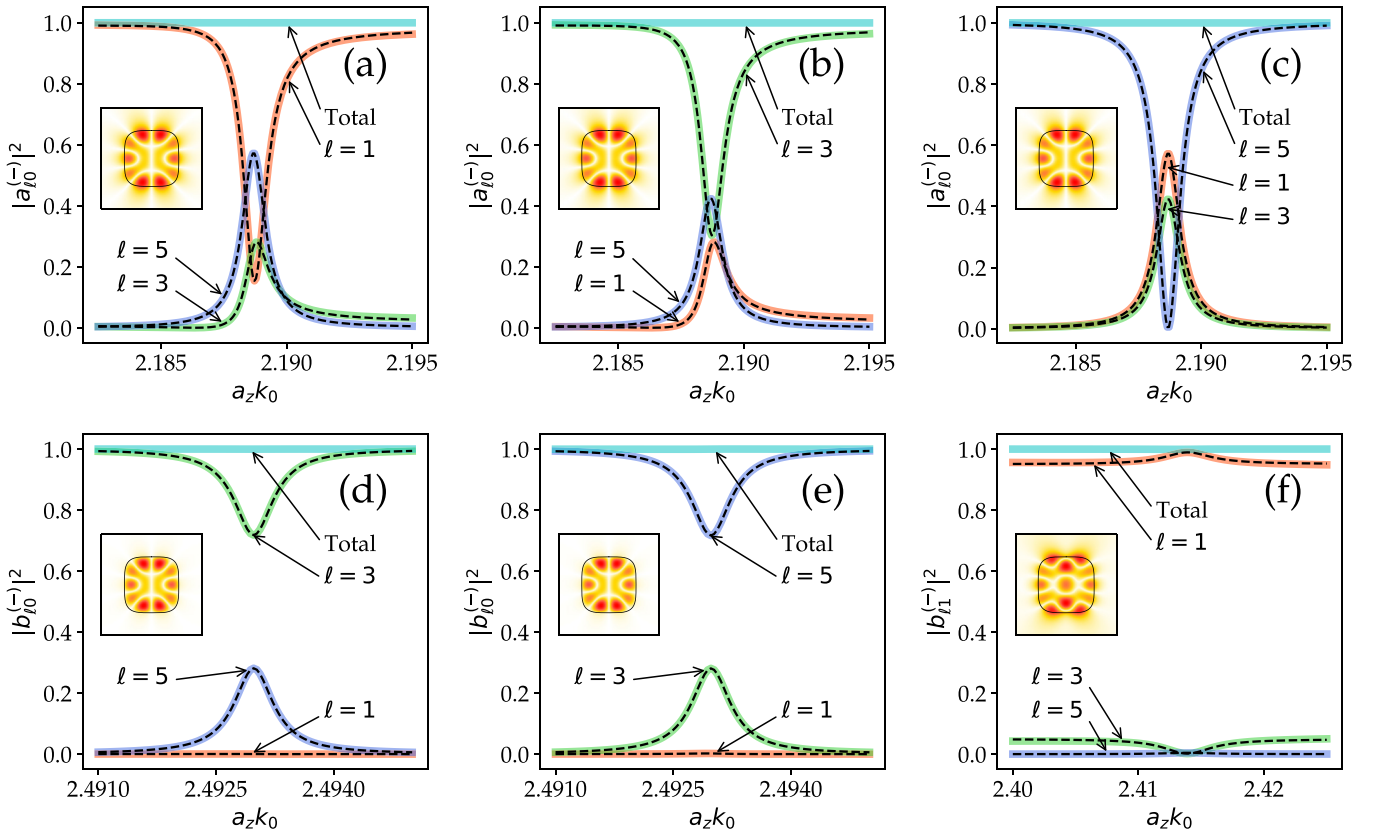$$\mathbf{c}_m^{(\mathrm{res})} = a\mathbf{c}_r, \tag{59}$$

FIG. 2. TCMT reflection coefficients as defined in Eq. (1) for a symmetric solid of revolution, $\alpha = 0$. (a)–(c) show the optical response from a transverse electric (TE) resonant mode $m = 0$, (d), (e) from a transverse magnetic (TM) mode $m = 0$, and (f) from a TM-like mode $m = 1$. The solid lines show the reflection coefficients to scattering channels specified by orbital number ℓ, as explained in (a). The thin black dashed line demonstrates the EBCM solutions. The field profiles of the resonant modes in the $x0z$ plane are shown in the insets as $|E_y|$ for (a)–(c) and $|H_y|$ for (e)–(g), $a_0/a_z = 0.9692$ for (a)–(e) and $a_0/a_z = 1$ for (f). The incident wave is TE polarized in (a)–(c) and TM polarized in (d)–(f). The parameters of the incident wave for each panel are as follows: (a) $\ell = 1$, $m = 0$, (b) $\ell = 3$, $m = 0$, (c) $\ell = 5$, $m = 0$, (d) $\ell = 3$, $m = 0$, (e) $\ell = 5$, $m = 0$, (f) $\ell = 1$, $m = 1$.

where $\mathbf{c}_r$ is the expansion vector of the TCMT resonant mode. From Eqs. (57) and (58) we have

$$\mathbf{c}_r = -i\sqrt{\frac{2u}{\alpha}}\boldsymbol{x}_r(\bar{\omega}). \qquad (60)$$

Notice that according to Eq. (52) we still have the freedom in choosing the phase of u. On the other hand, the TCMT resonant mode can be defined up to an arbitrary phase factor. In what follows we choose $\arg(u) = -\arg(\alpha)$, which yields

$$\mathbf{c}_r = \frac{-2i}{\alpha}\sqrt{\frac{\boldsymbol{y}_r^\dagger(\bar{\omega})\boldsymbol{y}_r(\bar{\omega})}{2\gamma}}\boldsymbol{x}_r(\bar{\omega}). \qquad (61)$$

VI. SUMMARY AND NUMERICAL VALIDATION

Before proceeding to a numerical validation we summarize our finding by providing a recipe for applying the TCMT decomposition of scattering spectra. Let us remind the reader that the sole motivation behind this paper is building up a simplified description of Fano resonances. Therefore, should a Fano resonance be observed in the SR scattering spectrum, the TCMT recipe goes in the following manner.

First, the scattering matrix $\widehat{S}_m(\bar{\omega})$ and the electromagnetic field within the SR, $\mathbf{c}_m(\bar{\omega})$, are computed by the EBCM at a certain frequency $\bar{\omega}$. There is no rigorous guidance for the value of $\bar{\omega}$. It is clear though that $\bar{\omega}$ has to be chosen within the frequency range of the Fano anomaly in the scattering spectrum. Second, the eigenvalue problem

$$\widehat{M}_m\boldsymbol{x}_r = \lambda_n\boldsymbol{x}_r,$$
$$\widehat{M}_m^\dagger\boldsymbol{y}_r = \lambda_r^*\boldsymbol{y}_r \qquad (62)$$

is solved for finding the smallest eigenvalue λ_r. The corresponding left and right eigenvectors are normalized according to

$$\boldsymbol{y}_r^\dagger\boldsymbol{x}_r = 1. \qquad (63)$$

Third, the parameter α is found from the following formula,

$$\alpha = \frac{\lambda_r(\bar{\omega}) - \lambda_r(\bar{\omega} + \Delta\omega)}{\Delta\omega}, \qquad (64)$$

where $\Delta\omega$ is a small increment of the incident frequency. The rest of the recipe is straightforward. All relevant quantities can be found through a step-by-step application of the formulas collected in Table I, which summarizes the findings of the previous sections.

To run the numerical test we took the SR surface given by the equation below,

$$\left(\frac{\sqrt{x^2 + y^2}}{a_0}\right)^4 + \left(\frac{z}{a_z}\right)^4 + \frac{z}{\alpha} = 1. \qquad (65)$$

We set the dielectric permittivity $\epsilon = 12$. For the first test we took a case symmetric with respect to $z \rightarrow -z$, i.e., $\alpha = 0$. The results of numerical simulations are shown in Fig. 2 where one can see a good agreement between the EBCM and the TCMT results. In Fig. 3 we demonstrate the numerical results for an asymmetric SR, $\alpha/a_z = 1.3333$. As one can see in Fig. 3, the TCMT again produces an accurate approximation of the EBCM data. In all the data presented one observes
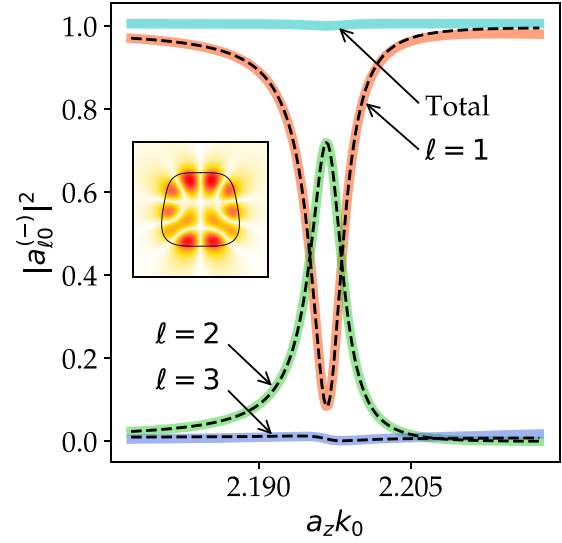

FIG. 3. TCMT for an asymmetric solid of revolution, $\alpha/a_z = 1.3333$, and $a_0/a_z = 0.9692$. The thick lines demonstrate the TCMT solution. The thick solid dashed lines show the EBCM solution for the reflection coefficients. The intensity profile of the resonant modes in the $x0z$ plane is shown in the inset as $|E_y|$. The incident wave is TE polarized. The parameters of the incident wave are $\ell = 1, m = 0$.

Lorentz line shapes. In Fig. 4 we present a case with asymmetric Fano line shapes. The Fano line shapes were obtained by exciting the resonance by a mixture of incident waves equally populating the first five channels $\ell = 1, 2, \ldots, 5$. The waves with $\ell = 2$ and $\ell = 4$ are not coupled to the resonance, resulting in a frequency-independent response. Therefore $a_{\ell,2}^{(-)}$ and $a_{\ell,4}^{(-)}$ are not shown in Fig. 4.
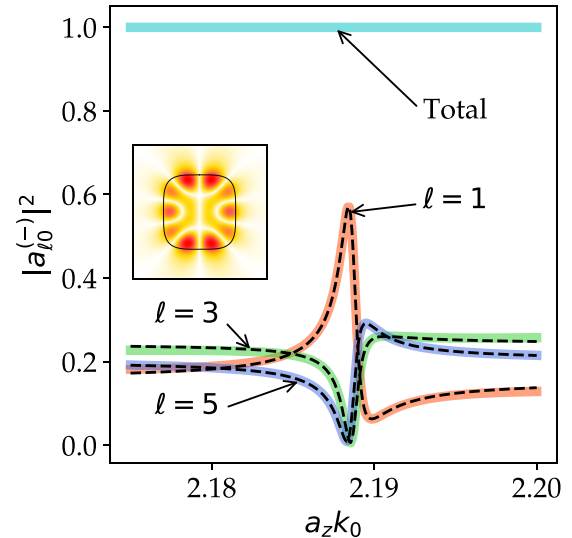

FIG. 4. TCMT for a symmetric solid of revolution, $\alpha/a_z = 0$, and $a_0/a_z = 0.9692$ with incoming waves injected into first five incident channels, $a_{\ell,0}^{(+)} = 0.4472$ if $\ell \leqslant 5$, and $a_{\ell,0}^{(+)} = 0$ if $\ell > 5$. The incident wave is TE polarized. The thick lines demonstrate the TCMT solution. The thick solid dashed lines show the EBCM solution for the reflection coefficients. The intensity profile of the resonant modes in the $x0z$ plane is shown in the inset as $|E_y|$.

VII. CONCLUSION

We propose a single resonance coupled-mode approach to light scattering by lossless dielectric solids of revolution, relying on the symmetries and energy conservation we derived the constraints imposed on the parameters of the temporal coupled mode equations. By using a biorthogonal decomposition of the S matrix found with the extended boundary condition method we derived all parameters required for application of the temporal coupled-mode theory, i.e., the resonant frequency, radiation decay rate, and coupling constants with incident and outgoing channels, in a closed form. The full list of formulas required for application of the temporal coupled-mode theory in combination with the extended boundary condition methods is presented in Table I. The proposed approach allows for constructing a frequency-dependent Fano response due to a single resonance after the full-wave solution has been found at a single incident frequency. The results demonstrate a good agreement as compared to full-wave simulations. It is found that the basic assumption leading to the single resonance coupled-mode theory is the frequency independence of all but one eigenvalue associated with the applied biorthogonal basis. This assumption can only hold true for an isolated resonance which does not overlap with the other neighboring resonances. The overlap leads to a violation of the TCMT constraint relating the coupling constants to the S-matrix nonresonant (background) scattering. In other words, the response due to the neighboring resonances cannot be fitted to a frequency-independent background. This problem could be solved by introducing a multimodal TCMT, such as in Ref. [18], which poses an interesting subject for future studies.

ACKNOWLEDGMENT

APPENDIX

The time-stationary solution of Eqs. (2) and (3) at incident frequency ω can be written in the form of the S matrix,

$$\widehat{S}_m = \widehat{B}_m + \frac{\mathbf{d}_m \boldsymbol{\kappa}_m^{\mathsf{T}}}{i\omega_0 - i\omega + \gamma}. \tag{A1}$$

The S matrix is unitary, thus, by using $\widehat{S}_m \widehat{S}_m^{\dagger} = \widehat{\mathbb{I}}$, we can find

$$\widehat{B}_m \boldsymbol{\kappa}_m^* + \frac{1}{2\gamma} (\boldsymbol{\kappa}_m^{\mathsf{T}} \boldsymbol{\kappa}_m^*) \mathbf{d}_m = 0. \tag{A2}$$

At the same time $\widehat{S}_m^{\dagger} \widehat{S}_m = \widehat{\mathbb{I}}$ yields

$$\widehat{B}_m^{\dagger} \mathbf{d}_m + \boldsymbol{\kappa}_m^* = 0, \tag{A3}$$

where we used $\mathbf{d}^{\dagger}\mathbf{d} = 2\gamma$. By multiplying Eq. (A2) with $\widehat{B}_m^{\dagger}$ from the left and applying Eq. (A3) we find

$$\boldsymbol{\kappa}_m^{\dagger} \boldsymbol{\kappa}_m = 2\gamma, \tag{A4}$$

and

$$\widehat{B}_m \boldsymbol{\kappa}_m^* = \mathbf{d}_m, \tag{A5}$$

where we used the unitarity of $\widehat{B}_m$.

Let us now use Eq. (13), which reads

$$\widehat{S}_m^{\mathsf{T}} = \widehat{J} \widehat{S}_m \widehat{J}, \tag{A6}$$

and apply the transpose operation to Eq. (A1). As a result we have

$$\widehat{B}_m^{\mathsf{T}} = \widehat{J} \widehat{B}_m \widehat{J}, \tag{A7}$$

and

$$\widehat{J} \boldsymbol{\kappa}_m \mathbf{d}_m^{\mathsf{T}} = \mathbf{d}_m \boldsymbol{\kappa}_m^{\mathsf{T}} \widehat{J}. \tag{A8}$$

By using Eqs. (A3) and (A7) we find

$$\widehat{B}_m \widehat{J} \mathbf{d}_m^* = -\widehat{J} \boldsymbol{\kappa}_m. \tag{A9}$$

The latter formula is equivalent to

$$\widehat{B}_m^{\dagger} \widehat{J} \boldsymbol{\kappa}_m = -\widehat{J} \mathbf{d}_m^*. \tag{A10}$$

In the next step we left multiply Eq. (A8) by $\widehat{B}_m^{\dagger}$. By virtue of Eqs. (A3) and (A10) we have

$$\mathbf{d}_m^* \mathbf{d}_m^{\mathsf{T}} = \widehat{J} \boldsymbol{\kappa}_m^* \boldsymbol{\kappa}_m^{\mathsf{T}} \widehat{J}, \tag{A11}$$

where we also applied $\widehat{J} = \widehat{J}^{-1}$. Now we multiply Eq. (A11) by $\mathbf{d}_m^{\mathsf{T}}$ from the left and $\mathbf{d}_m^*$ from the right. The result is

$$(2\gamma)^2 = (\mathbf{d}_m^{\mathsf{T}} \widehat{J} \boldsymbol{\kappa}_m^*)(\boldsymbol{\kappa}_m^{\mathsf{T}} \widehat{J} \mathbf{d}_m^*) = (\mathbf{d}_m^{\dagger} \widehat{J} \boldsymbol{\kappa}_m)^*(\mathbf{d}_m^{\dagger} \widehat{J} \boldsymbol{\kappa}_m), \tag{A12}$$

and consequently

$$\mathbf{d}_m^{\dagger} \widehat{J} \boldsymbol{\kappa}_m = 2\gamma e^{i\xi}, \tag{A13}$$

where ξ is an arbitrary phase. By multiplying Eq. (A11) by $\mathbf{d}_m^{\mathsf{T}}$ from the left and using Eq. (A13) we find

$$\boldsymbol{\kappa}_m = e^{i\xi} \widehat{J} \mathbf{d}_m \tag{A14}$$

The phase ξ can always be eliminated by multiplying the incident channel functions by $e^{i\xi/2}$ and the outgoing channel functions by $e^{-i\xi/2}$. Notice that the above multiplication is consistent with the time-reversal map between the incident and the outgoing channels, thus in what follows we set $\xi = 0$. Finally, we arrived at the following equations,

$$\widehat{B}_m \widehat{J} \mathbf{d}_m^* = -\mathbf{d}_m, \quad \boldsymbol{\kappa}_m = \widehat{J} \mathbf{d}_m. \tag{A15}$$

By applying the latter formula together with Eq. (A1) we end up with Eq. (18) from the main text.

[1] S. Kruk and Y. Kivshar, ACS Photonics **4**, 2638 (2017).

[2] J. H. Bahng, S. Jahani, D. G. Montjoy, T. Yao, N. Kotov, and A. Marandi, ACS Nano **14**, 17203 (2020).

[3] T. Liu, R. Xu, P. Yu, Z. Wang, and J. Takahara, Nanophotonics **9**, 1115 (2020).

[4] S. Krasikov, M. Odit, D. Dobrykh, I. Yusupov, A. Mikhailovskaya, D. Shakirova, A. Shcherbakov, A. Slobozhanyuk, P. Ginzburg, D. Filonov, and A. Bogdanov, Phys. Rev. Appl. **15**, 024052 (2021).

[5] Y. Kivshar, Nano Lett. **22**, 3513 (2022).

[6] M. I. Tribelsky, S. Flach, A. E. Miroshnichenko, A. V. Gorbach, and Y. S. Kivshar, Phys. Rev. Lett. **100**, 043903 (2008).

[7] M. V. Rybin, K. B. Samusev, I. S. Sinev, G. Semouchkin, E. Semouchkina, Y. S. Kivshar, and M. F. Limonov, Opt. Express **21**, 30107 (2013).

[8] M. F. Limonov, M. V. Rybin, A. N. Poddubny, and Y. S. Kivshar, Nat. Photonics **11**, 543 (2017).

[9] E. A. Muljarov and T. Weiss, Opt. Lett. **43**, 1978 (2018).

[10] P. Lalanne, W. Yan, K. Vynck, C. Sauvan, and J.-P. Hugonin, Laser Photonics Rev. **12**, 1700113 (2018).

[11] P. T. Kristensen, K. Herrmann, F. Intravaia, and K. Busch, Adv. Optics Photonics **12**, 612 (2020).

[12] M. Benzaouia, J. D. Joannopoulos, S. G. Johnson, and A. Karalis, Phys. Rev. Res. **3**, 033228 (2021).

[13] C. Sauvan, T. Wu, R. Zarouf, E. A. Muljarov, and P. Lalanne, Opt. Express **30**, 6846 (2022).

[14] L. Ge, Photonics Res. **5**, B20 (2017).

[15] J. S. T. Gongora, G. Favraud, and A. Fratalocchi, Nanotechnology **28**, 104001 (2017).

[16] S. Fan, W. Suh, and J. D. Joannopoulos, J. Opt. Soc. Am. A **20**, 569 (2003).

[17] Z. Zhao, C. Guo, and S. Fan, Phys. Rev. A **99**, 033839 (2019).

[18] W. Suh, Z. Wang, and S. Fan, IEEE J. Quantum Electron. **40**, 1511 (2004).

[19] Z. Ruan and S. Fan, Phys. Rev. A **85**, 043828 (2012).

[20] N. Avaritsiotis, T. Kamalakis, and T. Sphicopoulos, J. Lightwave Technol. **29**, 736 (2011).

[21] F. Alpeggiani, N. Parappurath, E. Verhagen, and L. Kuipers, Phys. Rev. X **7**, 021035 (2017).

[22] E. N. Bulgakov and D. N. Maksimov, J. Opt. Soc. Am. B **35**, 2443 (2018).

[23] W. Yan, R. Faggiani, and P. Lalanne, Phys. Rev. B **97**, 205422 (2018).

[24] K. Koshelev, Y. Tang, K. Li, D.-Y. Choi, G. Li, and Y. Kivshar, ACS Photonics **6**, 1639 (2019).

[25] M. Makarenko, A. Burguete-Lopez, F. Getman, and A. Fratalocchi, Sci. Rep. **10**, 9038 (2020).

[26] P. S. Pankin, D. N. Maksimov, K.-P. Chen, and I. V. Timofeev, Sci. Rep. **10**, 13691 (2020).

[27] M. I. Tribelsky and A. E. Miroshnichenko, Nanophotonics **10**, 4357 (2021).

[28] J. Ren, S. Franke, and S. Hughes, Phys. Rev. X **11**, 041020 (2021).

[29] H. Zhang and O. D. Miller, arXiv:2010.08650.

[30] F. M. Kahnert, J. J. Stamnes, and K. Stamnes, Appl. Opt. **40**, 3110 (2001).

[31] P. Barber and C. Yeh, Appl. Opt. **14**, 2864 (1975).

[32] I. Rotter, Phys. Rev. E **64**, 036213 (2001).

[33] https://rscf.ru/project/22-72-00102/.